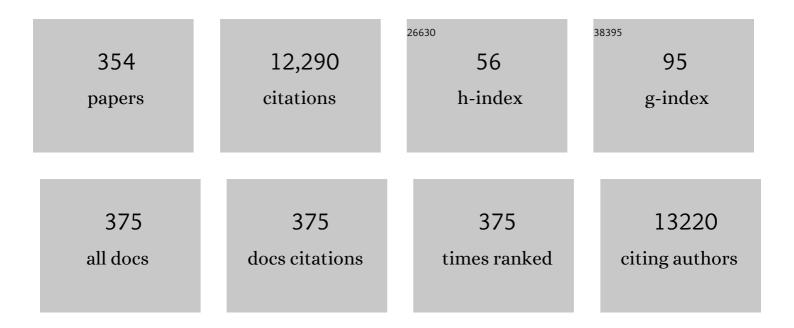
## Yubo Fan

List of Publications by Year in descending order

Source: https://exaly.com/author-pdf/4061993/publications.pdf Version: 2024-02-01



#	Article	IF	CITATIONS
1	Porous interbody fusion cage design via topology optimization and biomechanical performance analysis. Computer Methods in Biomechanics and Biomedical Engineering, 2023, 26, 650-659.	1.6	5
2	Hydrogel Loaded with VEGF/TFEBâ€Engineered Extracellular Vesicles for Rescuing Critical Limb Ischemia by a Dualâ€Pathway Activation Strategy. Advanced Healthcare Materials, 2022, 11, e2100334.	7.6	18
3	Biomechanics of adjacent segment after three-level lumbar fusion, hybrid single-level semi-rigid fixation with two-level lumbar fusion. Computer Methods in Biomechanics and Biomedical Engineering, 2022, 25, 455-463.	1.6	3
4	Effect of intermittent pneumatic compression with different inflation pressures on the distal microvascular responses of the foot in people with type 2 diabetes mellitus. International Wound Journal, 2022, 19, 968-977.	2.9	5
5	Phenytoin Regulates Migration and Osteogenic Differentiation by MAPK Pathway in Human Periodontal Ligament Cells. Cellular and Molecular Bioengineering, 2022, 15, 151-160.	2.1	8
6	Label-free visible colorimetric biosensor for detection of multiple pathogenic bacteria based on engineered polydiacetylene liposomes. Journal of Colloid and Interface Science, 2022, 606, 1684-1694.	9.4	18
7	A surface-eroding poly(1,3-trimethylene carbonate) coating for magnesium based cardiovascular stents with stable drug release and improved corrosion resistance. Bioactive Materials, 2022, 7, 144-153.	15.6	17
8	A review of magnetic ordered materials in biomedical field: Constructions, applications and prospects. Composites Part B: Engineering, 2022, 228, 109401.	12.0	16
9	The effect of periodic stretching on countering bone loss in hindlimb unloading rat. Acta Astronautica, 2022, 190, 202-207.	3.2	2
10	Near-infrared triggered injectable ferrimagnetic chitosan thermosensitive hydrogel for photo hyperthermia and precisely controlled drug release in tumor ablation. European Polymer Journal, 2022, 162, 110879.	5.4	16
11	Simulation of stent retriever thrombectomy in acute ischemic stroke by finite element analysis. Computer Methods in Biomechanics and Biomedical Engineering, 2022, 25, 740-749.	1.6	2
12	Variations of human cerebral and ocular blood flow during exposure to multi-axial accelerations. Medical and Biological Engineering and Computing, 2022, 60, 471-486.	2.8	1
13	Charge balancing stabilized apatite enter into collagen fibers by osmotic pressure to induce the formation of intrafibrillar mineralization. Materials Today Communications, 2022, 30, 103064.	1.9	3
14	Reconfigurable and regenerable liquid metal surface oxide for continuous and quantifiable adsorption of biological dye. Applied Materials Today, 2022, 26, 101265.	4.3	3
15	Oriented/dual-gradient in structure and mechanics chitosan hydrogel bio-films based on stretching for guiding cell orientation. Composites Part B: Engineering, 2022, 232, 109616.	12.0	8
16	The effects of titanium mesh cage size on the biomechanical responses of cervical spine after anterior cervical corpectomy and fusion: A finite element study. Clinical Biomechanics, 2022, 91, 105547.	1.2	12
17	Highâ€Throughput DNA Tensioner Platform for Interrogating Mechanical Heterogeneity of Single Living Cells. Small, 2022, 18, e2106196.	10.0	15
18	GNIFdb: a neoantigen intrinsic feature database for glioma. Database: the Journal of Biological Databases and Curation, 2022, 2022, .	3.0	5

#	Article	IF	CITATIONS
19	Engineer a preâ€metastatic niched microenvironment to attract breast cancer cells by utilizing a <scp>3D</scp> printed polycaprolactone/nanoâ€hydroxyapatite osteogenic scaffold – An in vitro model system for proof of concept. Journal of Biomedical Materials Research - Part B Applied Biomaterials, 2022, 110, 1604-1614.	3.4	6
20	Synergistically Detachable Microneedle Dressing for Programmed Treatment of Chronic Wounds. Advanced Healthcare Materials, 2022, 11, e2102180.	7.6	30
21	Selfâ€Organization of Tissue Growth by Interfacial Mechanical Interactions in Multilayered Systems. Advanced Science, 2022, 9, e2104301.	11.2	3
22	Study on the Influence of Shear Stress and Pulse Electrical Stimulation to the Growth of Cardiomyocytes. Journal of Biomedical Nanotechnology, 2022, 18, 132-143.	1.1	3
23	3D Segmentation Guided Style-Based Generative Adversarial Networks for PET Synthesis. IEEE Transactions on Medical Imaging, 2022, 41, 2092-2104.	8.9	8
24	Effect of Inter-Fragmentary Gap Size on Neovascularization During Bone Healing: A Micro-CT Imaging Study. Frontiers in Bioengineering and Biotechnology, 2022, 10, 808182.	4.1	0
25	Efficacy of various multi-layers of orthodontic clear aligners: a simulated study. Computer Methods in Biomechanics and Biomedical Engineering, 2022, 25, 1710-1721.	1.6	7
26	Differential Regulation by Mechanical Stretch of the Expressions of Large-Conductance Ca2+-Activated K+ Channel and L-Type Voltage-Dependent Ca2+ Channel in Rat Uterine Smooth Muscle Cells. Journal of Membrane Biology, 2022, 255, 357-361.	2.1	1
27	Prediction of Femoral Strength Based on Bone Density and Biochemical Markers in Elderly Men With Type 2 Diabetes Mellitus. Frontiers in Bioengineering and Biotechnology, 2022, 10, 855364.	4.1	2
28	Selfâ€Powered Gesture Recognition Wristband Enabled by Machine Learning for Full Keyboard and Multicommand Input. Advanced Materials, 2022, 34, e2200793.	21.0	81
29	Applying exercise-mimetic engineered skeletal muscle model to interrogate the adaptive response of irisin to mechanical force. IScience, 2022, 25, 104135.	4.1	2
30	Red blood cell-like magnetic particles and magnetic field promoted neuronal outgrowth by activating Netrin-1/DCC signaling pathway in vitro and in vivo. Composites Part B: Engineering, 2022, 237, 109789.	12.0	3
31	Differences in root stress and strain distribution in buccal and lingual orthodontics: A finite element analysis study. Medicine in Novel Technology and Devices, 2022, 14, 100119.	1.6	3
32	Non-contact electrical stimulation as an effective means to promote wound healing. Bioelectrochemistry, 2022, 146, 108108.	4.6	11
33	pH-responsive mesoporous Fe2O3–Au nanomedicine delivery system with magnetic targeting for cancer therapy. Medicine in Novel Technology and Devices, 2022, 15, 100127.	1.6	6
34	A systematic review of DVT and stent restenosis after stent implantation for iliac vein compression syndrome. Medicine in Novel Technology and Devices, 2022, 15, 100125.	1.6	0
35	Static magnetic field regulates proliferation, migration, and differentiation of human dental pulp stem cells by MAPK pathway. Cytotechnology, 2022, 74, 395-405.	1.6	2
36	Wearable Iontronic FMG for Classification of Muscular Locomotion. IEEE Journal of Biomedical and Health Informatics, 2022, 26, 2854-2863.	6.3	4

#	Article	IF	CITATIONS
37	Ultracompact Deep Neural Network for Ultrafast Optical Property Extraction in Spatial Frequency Domain Imaging (SFDI). Photonics, 2022, 9, 327.	2.0	2
38	Study on the effects of alternating capacitive electric fields with different frequencies on promoting wound healing. Medicine in Novel Technology and Devices, 2022, 16, 100142.	1.6	3
39	Cytosolic peptides encoding CaV1 C-termini downregulate the calcium channel activity-neuritogenesis coupling. Communications Biology, 2022, 5, 484.	4.4	6
40	A Self-Powered Optogenetic System for Implantable Blood Glucose Control. Research, 2022, 2022, .	5.7	7
41	In vitro fluidic systems: Applying shear stress on endothelial cells. Medicine in Novel Technology and Devices, 2022, 15, 100143.	1.6	10
42	Dual-phase injectable thermosensitive hydrogel incorporating Fe3O4@PDA with pH and NIR triggered drug release for synergistic tumor therapy. European Polymer Journal, 2022, 176, 111424.	5.4	10
43	Novel Mg-Ca-La alloys for guided bone regeneration: Mechanical performance, stress corrosion behavior and biocompatibility. Materials Today Communications, 2022, 32, 103949.	1.9	4
44	Aligned graphene/silk fibroin conductive fibrous scaffolds for guiding neurite outgrowth in rat spinal cord neurons. Journal of Biomedical Materials Research - Part A, 2021, 109, 488-499.	4.0	14
45	Threeâ€dimensional silk fibroin scaffolds incorporated with graphene for bone regeneration. Journal of Biomedical Materials Research - Part A, 2021, 109, 515-523.	4.0	19
46	Bilayer nicorandil-loaded small-diameter vascular grafts improve endothelial cell function via PI3K/AKT/eNOS pathway. Bio-Design and Manufacturing, 2021, 4, 72-86.	7.7	4
47	Idealized conductance: A new method to evaluate stiffness of trabecular bone. International Journal for Numerical Methods in Biomedical Engineering, 2021, 37, e3425.	2.1	4
48	Refreshable Braille Display System Based on Triboelectric Nanogenerator and Dielectric Elastomer. Advanced Functional Materials, 2021, 31, 2006612.	14.9	96
49	Nanopharmaceutical-based regenerative medicine: a promising therapeutic strategy for spinal cord injury. Journal of Materials Chemistry B, 2021, 9, 2367-2383.	5.8	7
50	Flow shear stress controls the initiation of neovascularization <i>via</i> heparan sulfate proteoglycans within a biomimetic microfluidic model. Lab on A Chip, 2021, 21, 421-434.	6.0	17
51	<i>In vitro</i> degradation, biocompatibility and antibacterial properties of pure zinc: assessing the potential of Zn as a guided bone regeneration membrane. Journal of Materials Chemistry B, 2021, 9, 5114-5127.	5.8	22
52	The cushioning function of woodpecker's jaw apparatus during the pecking process. Computer Methods in Biomechanics and Biomedical Engineering, 2021, 24, 527-537.	1.6	6
53	Biological analysis of woodpecker's brain after impact experiments. Science China Technological Sciences, 2021, 64, 1101-1106.	4.0	5
54	An Optical Method for Immediate Evaluation of Microfoam Stability in Foam Sclerotherapy. Skin Pharmacology and Physiology, 2021, 34, 128-134.	2.5	0

#	Article	IF	CITATIONS
55	A biomimetic hierarchical small intestinal submucosa–chitosan sponge/chitosan hydrogel scaffold with a micro/nano structure for dural repair. Journal of Materials Chemistry B, 2021, 9, 7821-7834.	5.8	21
56	Molecular insights into MXene destructing the cell membrane as a "nano thermal blade― Physical Chemistry Chemical Physics, 2021, 23, 3341-3350.	2.8	21
57	Mechano-Sensing and shear stress-shielding by endothelial primary cilia: structure, composition, and function. Biocell, 2021, 45, 1187-1199.	0.7	3
58	An Index From Transcranial Doppler Signals for Evaluation of Stroke Rehabilitation Using External Counterpulsation. IEEE Transactions on Neural Systems and Rehabilitation Engineering, 2021, 29, 1487-1493.	4.9	2
59	Microfluidic chips for the endothelial biomechanics and mechanobiology of the vascular system. Biocell, 2021, 45, 797-811.	0.7	4
60	Effects of reverse deployment of cone-shaped vena cava filter on improvements in hemodynamic performance in vena cava. BioMedical Engineering OnLine, 2021, 20, 19.	2.7	1
61	Influence of renal artery stenosis morphology on hemodynamics. Computer Methods in Biomechanics and Biomedical Engineering, 2021, 24, 1294-1301.	1.6	4
62	Subjective assessment on visual fatigue versus stereoscopic disparities. Journal of the Society for Information Display, 2021, 29, 497-504.	2.1	8
63	Effect of different thermal stimuli on improving microcirculation in the contralateral foot. BioMedical Engineering OnLine, 2021, 20, 14.	2.7	5
64	Influence of Distal Re-entry Tears on False Lumen Thrombosis After Thoracic Endovascular Aortic Repair in Type B Aortic Dissection Patients: A Computational Fluid Dynamics Simulation. Cardiovascular Engineering and Technology, 2021, 12, 426-437.	1.6	7
65	Stimulation of vascular smooth muscle cell proliferation by stiff matrix via the IK <sub>Ca</sub> channelâ€dependent Ca <sup>2+</sup> signaling. Journal of Cellular Physiology, 2021, 236, 6897-6906.	4.1	5
66	Effect of the medial collateral ligament and the lateral ulnar collateral ligament injury on elbow stability: a finite element analysis. Computer Methods in Biomechanics and Biomedical Engineering, 2021, 24, 1517-1529.	1.6	2
67	Microcracks on the Rat Root Surface Induced by Orthodontic Force, Crack Extension Simulation, and Proteomics Study. Annals of Biomedical Engineering, 2021, 49, 2228-2242.	2.5	3
68	Low-Cost and Scalable Platform with Multiplexed Microwell Array Biochip for Rapid Diagnosis of COVID-19. Research, 2021, 2021, 2813643.	5.7	13
69	Biochemical and Morphological Abnormalities of Subchondral Bone and Their Association with Cartilage Degeneration in Spontaneous Osteoarthritis. Calcified Tissue International, 2021, 109, 179-189.	3.1	7
70	Electrical Stimulation Promotes Stem Cell Neural Differentiation in Tissue Engineering. Stem Cells International, 2021, 2021, 1-14.	2.5	40
71	Flow-mediated dilation analysis coupled with nitric oxide transport to enhance the assessment of endothelial function. Journal of Applied Physiology, 2021, 131, 1-14.	2.5	6
72	Finite element analysis of lumbar spine with different backpack positions in parachuting landing. Computer Methods in Biomechanics and Biomedical Engineering, 2021, 24, 1-8.	1.6	1

#	Article	IF	CITATIONS
73	Microfluidic Model to Mimic Initial Event of Neovascularization. Journal of Visualized Experiments, 2021, , .	0.3	1
74	Microstructural and mechanical evaluations of region segmentation methods in classifications of osteonecrosis. Journal of Biomechanics, 2021, 119, 110208.	2.1	1
75	Patientâ€Specific Organoid and Organâ€onâ€aâ€Chip: 3D Cellâ€Culture Meets 3D Printing and Numerical Simulation. Advanced Biology, 2021, 5, e2000024.	2.5	31
76	Studies on preparation and formation mechanism of poly(lactide-co-glycolide) microrods via one-step electrospray and an application for drug delivery system. European Polymer Journal, 2021, 148, 110372.	5.4	22
77	Gastrointestinal Microenvironment and the Gut-Lung Axis in the Immune Responses of Severe COVID-19. Frontiers in Molecular Biosciences, 2021, 8, 647508.	3.5	9
78	Cell membrane-biomimetic coating via click-mediated liposome fusion for mitigating the foreign-body reaction. Biomaterials, 2021, 271, 120768.	11.4	17
79	Dynamic real-time imaging of living cell traction force by piezo-phototronic light nano-antenna array. Science Advances, 2021, 7, .	10.3	65
80	Cyclic Strain and Electrical Co-stimulation Improve Neural Differentiation of Marrow-Derived Mesenchymal Stem Cells. Frontiers in Cell and Developmental Biology, 2021, 9, 624755.	3.7	10
81	Investigation of failure modes of explanted porcine valves in the mitral position. Journal of Thoracic Disease, 2021, 13, 2858-2866.	1.4	0
82	A personalized 3D-printed plate for tibiotalocalcaneal arthrodesis: Design, fabrication, biomechanical evaluation and postoperative assessment. Computers in Biology and Medicine, 2021, 133, 104368.	7.0	16
83	A Review: Optimization for Poly(glycerol sebacate) and Fabrication Techniques for Its Centered Scaffolds. Macromolecular Bioscience, 2021, 21, e2100022.	4.1	20
84	The characteristics of distal tears affect false lumen thrombosis rate after thoracic endovascular aortic repair for acute type B dissection. Interactive Cardiovascular and Thoracic Surgery, 2021, 33, 755-762.	1.1	0
85	Biomechanical design and analysis of auxetic pedicle screw to resist loosening. Computers in Biology and Medicine, 2021, 133, 104386.	7.0	23
86	Macrophage Polarization in Response to Biomaterials for Vascularization. Annals of Biomedical Engineering, 2021, 49, 1992-2005.	2.5	12
87	neoDL: a novel neoantigen intrinsic feature-based deep learning model identifies IDH wild-type glioblastomas with the longest survival. BMC Bioinformatics, 2021, 22, 382.	2.6	3
88	Hydrogel-based therapeutic angiogenesis: An alternative treatment strategy for critical limb ischemia. Biomaterials, 2021, 274, 120872.	11.4	20
89	Evaluation methods for mechanical biocompatibility of hernia repair meshes: respective characteristics, application scope and future perspectives. Journal of Materials Research and Technology, 2021, 13, 1826-1840.	5.8	6
90	Preparation of Magnetic–Luminescent Bifunctional Rapeseed Pod-Like Drug Delivery System for Sequential Release of Dual Drugs. Pharmaceutics, 2021, 13, 1116.	4.5	7

#	Article	IF	CITATIONS
91	Two-dimensional dynamic walking stability of elderly females with a history of falls. Medical and Biological Engineering and Computing, 2021, 59, 1575-1583.	2.8	2
92	A Bioresorbable Dynamic Pressure Sensor for Cardiovascular Postoperative Care. Advanced Materials, 2021, 33, e2102302.	21.0	85
93	A biomimetic triple-layered biocomposite with effective multifunction for dura repair. Acta Biomaterialia, 2021, 130, 248-267.	8.3	14
94	Stereotactic technology for 3D bioprinting: from the perspective of robot mechanism. Biofabrication, 2021, 13, 043001.	7.1	8
95	Biomechanical study on implantable and interventional medical devices. Acta Mechanica Sinica/Lixue Xuebao, 2021, 37, 875-894.	3.4	19
96	Full-field strain mapping for characterization of structure-related variation in corneal biomechanical properties using digital image correlation (DIC) technology. Medicine in Novel Technology and Devices, 2021, 11, 100086.	1.6	1
97	A critical review on the biomechanical study of cervical interbody fusion cage. Medicine in Novel Technology and Devices, 2021, 11, 100070.	1.6	18
98	Soft substrate and decreased cytoskeleton contractility promote coupling and morphology maintenance of pluripotent stem cells. Acta Mechanica Sinica/Lixue Xuebao, 2021, 37, 1520-1529.	3.4	1
99	Self-powered technology for next-generation biosensor. Science Bulletin, 2021, 66, 1709-1712.	9.0	32
100	The differences between surface degradation and bulk degradation of FEM on the prediction of the degradation time for poly (lactic-co-glycolic acid) stent. Computer Methods in Biomechanics and Biomedical Engineering, 2021, , 1-8.	1.6	1
101	Multiomics Analysis Reveals the Prognostic Non-tumor Cell Landscape in Glioblastoma Niches. Frontiers in Genetics, 2021, 12, 741325.	2.3	0
102	Comparative study on hemodynamic environments around patient-specific carotid atherosclerotic plaques with different symmetrical features. Medicine in Novel Technology and Devices, 2021, 11, 100079.	1.6	3
103	Surface modification of electrospun fibers with mechano-growth factor for mitigating the foreign-body reaction. Bioactive Materials, 2021, 6, 2983-2998.	15.6	27
104	Fluid-induced corrosion behavior of degradable zinc for stent application. Journal of Materials Science and Technology, 2021, 91, 134-147.	10.7	12
105	Three-dimensional magnetic fibrous scaffold with icariin expanded by supercritical CO2 for bone tissue engineering under static magnetic field. Composites Part B: Engineering, 2021, 226, 109304.	12.0	16
106	Design of Robot-Assisted Task Involving Visuomotor Conflict for Identification of Proprioceptive Acuity. IEEE Transactions on Instrumentation and Measurement, 2021, 70, 1-10.	4.7	4
107	Vascular transplantation with dual-biofunctional ePTFE vascular grafts in a porcine model. Journal of Materials Chemistry B, 2021, 9, 7409-7422.	5.8	6
108	Human locomotion-control brain networks detected with independent component analysis. Journal of Integrative Neuroscience, 2021, 20, 695.	1.7	1

**Υυβο Γα**ν

#	Article	IF	CITATIONS
109	Triboelectric nanogenerator based on degradable materials. EcoMat, 2021, 3, e12072.	11.9	108
110	Direct mapping from diffuse reflectance to chromophore concentrations in multi-fx spatial frequency domain imaging (SFDI) with a deep residual network (DRN). Biomedical Optics Express, 2021, 12, 433.	2.9	18
111	Exploring the match between the degradation of the ECM-based composites and tissue remodeling in a full-thickness abdominal wall defect model. Biomaterials Science, 2021, 9, 7895-7910.	5.4	9
112	Detections of Steady-State Visual Evoked Potential and Simultaneous Jaw Clench Action from Identical Occipital Electrodes: A Hybrid Brain-Computer Interface Study. Journal of Medical and Biological Engineering, 2021, 41, 914-923.	1.8	0
113	Effect of Vibration on Alleviating Foot Pressure-Induced Ischemia under Occlusive Compression. Journal of Healthcare Engineering, 2021, 2021, 1-9.	1.9	Ο
114	A simple indentation technique for identifying localized liquefaction of the vitreous body. Journal of Biomechanics, 2021, 129, 110795.	2.1	1
115	Brainstem fMRI. Encyclopedia, 2021, 1, 4-11.	4.5	Ο
116	Multifunctional Switchable Nanocoated Membranes for Efficient Integrated Purification of Oil/Water Emulsions. ACS Applied Materials & Interfaces, 2021, 13, 54315-54323.	8.0	24
117	A rapid procedure for bacterial identification and antimicrobial susceptibility testing directly from positive blood cultures. Analyst, The, 2021, 147, 147-154.	3.5	5
118	Effect of Exercise Volume on Plantar Microcirculation and Tissue Hardness in People With Type 2 Diabetes. Frontiers in Bioengineering and Biotechnology, 2021, 9, 732628.	4.1	5
119	Delivery of Nitric Oxide in the Cardiovascular System: Implications for Clinical Diagnosis and Therapy. International Journal of Molecular Sciences, 2021, 22, 12166.	4.1	15
120	Effect of limb rotation on radiographic alignment measurement in mal-aligned knees. BioMedical Engineering OnLine, 2021, 20, 119.	2.7	3
121	Halftone spatial frequency domain imaging enables kilohertz high-speed label-free non-contact quantitative mapping of optical properties for strongly turbid media. Light: Science and Applications, 2021, 10, 245.	16.6	9
122	Blood flow patterns regulate PCSK9 secretion via MyD88-mediated pro-inflammatory cytokines. Cardiovascular Research, 2020, 116, 1721-1732.	3.8	42
123	A numerical method for guiding the design of surgical meshes with suitable mechanical properties for specific abdominal hernias. Computers in Biology and Medicine, 2020, 116, 103531.	7.0	9
124	Influence of multi-angle input of intraoperative fluoroscopic images on the spatial positioning accuracy of the C-arm calibration-based algorithm of a CAOS system. Medical and Biological Engineering and Computing, 2020, 58, 559-572.	2.8	3
125	Terminal Group Modification of Carbon Nanotubes Determines Covalently Bound Osteogenic Peptide Performance. ACS Biomaterials Science and Engineering, 2020, 6, 865-878.	5.2	15
126	A novel auxetic structure based bone screw design: Tensile mechanical characterization and pullout fixation strength evaluation. Materials and Design, 2020, 188, 108424.	7.0	54

#	Article	IF	CITATIONS
127	Biomimetic SIS-based biocomposites with improved biodegradability, antibacterial activity and angiogenesis for abdominal wall repair. Materials Science and Engineering C, 2020, 109, 110538.	7.3	30
128	Nestable arched triboelectric nanogenerator for large deflection biomechanical sensing and energy harvesting. Nano Energy, 2020, 69, 104417.	16.0	47
129	Polysaccharideâ€Peptide Cryogels for Multidrugâ€Resistantâ€Bacteria Infected Wound Healing and Hemostasis. Advanced Healthcare Materials, 2020, 9, e1901041.	7.6	69
130	Mechanical properties, degradation behaviors and biocompatibility of micro-alloyed Mg-Sr-RE alloys for stent applications. Materials Letters, 2020, 264, 127285.	2.6	17
131	Influence of Configuration on Stress Distribution of Pulmonary Monocusp Leaflet. Cardiovascular Engineering and Technology, 2020, 11, 134-140.	1.6	0
132	Reversible Conversion between Schottky and Ohmic Contacts for Highly Sensitive, Multifunctional Biosensors. Advanced Functional Materials, 2020, 30, 1907999.	14.9	61
133	Applications of decellularized materials in tissue engineering: advantages, drawbacks and current improvements, and future perspectives. Journal of Materials Chemistry B, 2020, 8, 10023-10049.	5.8	63
134	Spatiotemporal transfer of nitric oxide in patient-specific atherosclerotic carotid artery bifurcations with MRI and computational fluid dynamics modeling. Computers in Biology and Medicine, 2020, 125, 104015.	7.0	7
135	Improving Chronic Diabetic Wound Healing through an Injectable and Self-Healing Hydrogel with Platelet-Rich Plasma Release. ACS Applied Materials & Interfaces, 2020, 12, 55659-55674.	8.0	99
136	Electrochemically Enabled Embedded Three-Dimensional Printing of Freestanding Gallium Wire-like Structures. ACS Applied Materials & Interfaces, 2020, 12, 53966-53972.	8.0	30
137	Applications of materials for dural reconstruction in pre-clinical and clinical studies: Advantages and drawbacks, efficacy, and selections. Materials Science and Engineering C, 2020, 117, 111326.	7.3	22
138	Gender differences of morphological and hemodynamic characteristics of abdominal aortic aneurysm. Biology of Sex Differences, 2020, 11, 41.	4.1	5
139	Rapid Detection of mecA and femA Genes by Loop-Mediated Isothermal Amplification in a Microfluidic System for Discrimination of Different Staphylococcal Species and Prediction of Methicillin Resistance. Frontiers in Microbiology, 2020, 11, 1487.	3.5	15
140	Deep learning in digital pathology image analysis: a survey. Frontiers of Medicine, 2020, 14, 470-487.	3.4	77
141	Root surface microcracks induced by orthodontic force as a potential primary indicator of root resorption. Journal of Biomechanics, 2020, 110, 109938.	2.1	4
142	Biological and Physical Properties of a Modification Silicone Liner. IOP Conference Series: Materials Science and Engineering, 2020, 774, 012110.	0.6	2
143	Functional MRI Reveals Locomotion-Control Neural Circuits in Human Brainstem. Brain Sciences, 2020, 10, 757.	2.3	6
144	Brainstem Encephalitis Caused by Listeria monocytogenes. Pathogens, 2020, 9, 715.	2.8	15

#	Article	IF	CITATIONS
145	A micropore array-based solid lift-off method for highly efficient and controllable cell alignment and spreading. Microsystems and Nanoengineering, 2020, 6, 86.	7.0	9
146	Changes in the Kinematic and Kinetic Characteristics of Lunge Footwork during the Fatiguing Process. Applied Sciences (Switzerland), 2020, 10, 8703.	2.5	4
147	The Effect of TiAl6V4 Particles on Tissue in Rats. Journal of Physics: Conference Series, 2020, 1637, 012104.	0.4	0
148	The role of hemoglobin in nitric oxide transport in vascular system. Medicine in Novel Technology and Devices, 2020, 5, 100034.	1.6	11
149	Double coating of graphene oxide–polypyrrole on silk fibroin scaffolds for neural tissue engineering. Journal of Bioactive and Compatible Polymers, 2020, 35, 216-227.	2.1	11
150	Endothelial Progenitor Cellâ€Đerived Extracellular Vesicles: A Novel Candidate for Regenerative Medicine and Disease Treatment. Advanced Healthcare Materials, 2020, 9, e2000255.	7.6	33
151	InÂVivo Disintegration and Bioresorption of a Nacre-Inspired Graphene-Silk Film Caused by the Foreign-Body Reaction. IScience, 2020, 23, 101155.	4.1	8
152	Triboelectric-polarization-enhanced high sensitive ZnO UV sensor. Nano Today, 2020, 33, 100873.	11.9	33
153	A flexible self-arched biosensor based on combination of piezoelectric and triboelectric effects. Applied Materials Today, 2020, 20, 100699.	4.3	45
154	Emerging Implantable Energy Harvesters and Self-Powered Implantable Medical Electronics. ACS Nano, 2020, 14, 6436-6448.	14.6	223
155	The effects of silk layer-by-layer surface modification on the mechanical and structural retention of extracellular matrix scaffolds. Biomaterials Science, 2020, 8, 4026-4038.	5.4	19
156	A moisturizing chitosan-silk fibroin dressing with silver nanoparticles-adsorbed exosomes for repairing infected wounds. Journal of Materials Chemistry B, 2020, 8, 7197-7212.	5.8	58
157	NLRP3 inflammasome <i>via</i> IL-1β regulates PCSK9 secretion. Theranostics, 2020, 10, 7100-7110.	10.0	51
158	Human Motion Driven Self-Powered Photodynamic System for Long-Term Autonomous Cancer Therapy. ACS Nano, 2020, 14, 8074-8083.	14.6	77
159	Magnetic nanoparticles applied in targeted therapy and magnetic resonance imaging: crucial preparation parameters, indispensable pre-treatments, updated research advancements and future perspectives. Journal of Materials Chemistry B, 2020, 8, 5973-5991.	5.8	26
160	A wearable noncontact freeâ€rotating hybrid nanogenerator for selfâ€powered electronics. InformaÄnÃ- Materiály, 2020, 2, 1191-1200.	17.3	71
161	In vitro and in vivo degradation behavior of Mg–2Sr–Ca and Mg–2Sr–Zn alloys. Bioactive Materials, 2020, 5, 275-285.	15.6	58
162	A resazurin-based, nondestructive assay for monitoring cell proliferation during a scaffold-based 3D culture process. International Journal of Energy Production and Management, 2020, 7, 271-281.	3.7	21

#	Article	IF	CITATIONS
163	Emerging technologies for the prevention and management of diabetic foot ulcers. Journal of Tissue Viability, 2020, 29, 61-68.	2.0	36
164	Biomechanical influence of anchorages on orthodontic space closing mechanics by sliding method. Medical and Biological Engineering and Computing, 2020, 58, 1091-1097.	2.8	7
165	Effect of strain on degradation behaviors of WE43, Fe and Zn wires. Acta Biomaterialia, 2020, 113, 627-645.	8.3	52
166	Biomechanical effects of over lordotic curvature after spinal fusion on adjacent intervertebral discs under continuous compressive load. Clinical Biomechanics, 2020, 73, 149-156.	1.2	6
167	A 25-year bibliometric study of implantable energy harvesters and self-powered implantable medical electronics researches. Materials Today Energy, 2020, 16, 100386.	4.7	58
168	On-chip multiplexed single-cell patterning and controllable intracellular delivery. Microsystems and Nanoengineering, 2020, 6, 2.	7.0	37
169	A Hybrid Biofuel and Triboelectric Nanogenerator for Bioenergy Harvesting. Nano-Micro Letters, 2020, 12, 50.	27.0	41
170	A critical role of the K <sub>Ca</sub> 3.1 channel in mechanical stretchâ€induced proliferation of rat bone marrowâ€derived mesenchymal stem cells. Journal of Cellular and Molecular Medicine, 2020, 24, 3739-3744.	3.6	12
171	Promotion of Neuronal Guidance Growth by Aminated Graphene Oxide via Netrin-1/Deleted in Colorectal Cancer Signaling. ACS Chemical Neuroscience, 2020, 11, 604-614.	3.5	8
172	Flexible and stretchable dual mode nanogenerator for rehabilitation monitoring and information interaction. Journal of Materials Chemistry B, 2020, 8, 3647-3654.	5.8	47
173	Biomechanical effects of corticotomy facilitated orthodontic anterior retraction: a 3-dimensional finite element analysis. Computer Methods in Biomechanics and Biomedical Engineering, 2020, 23, 295-302.	1.6	3
174	Influence of the mechanical properties of biomaterials on degradability, cell behaviors and signaling pathways: current progress and challenges. Biomaterials Science, 2020, 8, 2714-2733.	5.4	111
175	The Biomechanical Relationship between Hallux Valgus Deformity and Metatarsal Pain. Journal of Healthcare Engineering, 2020, 2020, 1-7.	1.9	8
176	Ternary hydrogels with tunable mechanical and self-healing properties based on the synergistic effects of multiple dynamic bonds. Journal of Materials Chemistry B, 2020, 8, 4660-4671.	5.8	18
177	Effect of Electrospun Silk Fibroin–Silk Sericin Films on Macrophage Polarization and Vascularization. ACS Biomaterials Science and Engineering, 2020, 6, 3502-3512.	5.2	32
178	Highly aligned hierarchical intrafibrillar mineralization of collagen induced by periodic fluid shear stress. Journal of Materials Chemistry B, 2020, 8, 2562-2572.	5.8	38
179	A Batteryâ€Like Selfâ€Charge Universal Module for Motional Energy Harvest. Advanced Energy Materials, 2019, 9, 1901875.	19.5	68
180	Simulation Analysis of Trajectory Planning for Robot-Assisted Stereotactically Biological Printing. Lecture Notes in Computer Science, 2019, , 154-162.	1.3	2

#	Article	IF	CITATIONS
181	Small intestinal submucosa: superiority, limitations and solutions, and its potential to address bottlenecks in tissue repair. Journal of Materials Chemistry B, 2019, 7, 5038-5055.	5.8	64
182	EFFECTS OF ALVEOLAR MORPHOLOGY ON ALVEOLAR MECHANICS: AN EXPERIMENTAL STUDY OF MOUSE LUNG BASED ON TWO- AND THREE-DIMENSIONAL IMAGING METHODS. Journal of Mechanics in Medicine and Biology, 2019, 19, 1950027.	0.7	0
183	Lower limb joint motion and muscle force in treadmill and over-ground exercise. BioMedical Engineering OnLine, 2019, 18, 89.	2.7	22
184	Promoting Proliferation and Differentiation of Pre-Osteoblasts MC3T3-E1 Cells Under Combined Mechanical and Electrical Stimulation. Journal of Biomedical Nanotechnology, 2019, 15, 921-929.	1.1	8
185	Fabrication of Concentric Carbon Nanotube Rings and Their Application on Regulating Cell Growth. ACS Omega, 2019, 4, 16209-16216.	3.5	6
186	Biomechanical studies on biomaterial degradation and co-cultured cells: mechanisms, potential applications, challenges and prospects. Journal of Materials Chemistry B, 2019, 7, 7439-7459.	5.8	33
187	Fully Bioabsorbable Capacitor as an Energy Storage Unit for Implantable Medical Electronics. Advanced Science, 2019, 6, 1801625.	11.2	106
188	Degradation and biocompatibility of a series of strontium substituted hydroxyapatite coatings on magnesium alloys. RSC Advances, 2019, 9, 15013-15021.	3.6	20
189	Role of intraluminal thrombus in abdominal aortic aneurysm ruptures: A hemodynamic point of view. Medical Physics, 2019, 46, 4263-4275.	3.0	26
190	Incorporation of multi-walled carbon nanotubes to PMMA bone cement improves cytocompatibility and osseointegration. Materials Science and Engineering C, 2019, 103, 109823.	7.3	36
191	A bionic stretchable nanogenerator for underwater sensing and energy harvesting. Nature Communications, 2019, 10, 2695.	12.8	413
192	Evaluation and Prediction of Mass Transport Properties for Porous Implant with Different Unit Cells: A Numerical Study. BioMed Research International, 2019, 2019, 1-11.	1.9	5
193	Biodegradable Magnesium-Incorporated Poly( <scp>l</scp> -lactic acid) Microspheres for Manipulation of Drug Release and Alleviation of Inflammatory Response. ACS Applied Materials & Interfaces, 2019, 11, 23546-23557.	8.0	59
194	Conductive nanostructured Si biomaterials enhance osteogeneration through electrical stimulation. Materials Science and Engineering C, 2019, 103, 109748.	7.3	29
195	Diagonal-symmetrical and Midline-symmetrical Unit Cells with Same Porosity for Bone Implant: Mechanical Properties Evaluation. Journal of Bionic Engineering, 2019, 16, 468-479.	5.0	11
196	Apatite minerals derived from collagen phosphorylation modification induce the hierarchical intrafibrillar mineralization of collagen fibers. Journal of Biomedical Materials Research - Part A, 2019, 107, 2403-2413.	4.0	28
197	Design of Virtual Guiding Tasks With Haptic Feedback for Assessing the Wrist Motor Function of Patients With Upper Motor Neuron Lesions. IEEE Transactions on Neural Systems and Rehabilitation Engineering, 2019, 27, 984-994.	4.9	19
198	Body-Integrated Self-Powered System for Wearable and Implantable Applications. ACS Nano, 2019, 13, 6017-6024.	14.6	142

#	Article	IF	CITATIONS
199	Symbiotic cardiac pacemaker. Nature Communications, 2019, 10, 1821.	12.8	429
200	<i>In vivo</i> measurements of collapse behavior of human internal jugular vein during head-up tilt tests. Physiological Measurement, 2019, 40, 075006.	2.1	9
201	Research Methods and Progress of Patellofemoral Joint Kinematics: A Review. Journal of Healthcare Engineering, 2019, 2019, 1-13.	1.9	23
202	Wearable and Implantable Triboelectric Nanogenerators. Advanced Functional Materials, 2019, 29, 1808820.	14.9	296
203	Effects of Local Vibration With Different Intermittent Durations on Skin Blood Flow Responses in Diabetic People. Frontiers in Bioengineering and Biotechnology, 2019, 7, 310.	4.1	21
204	Shear Stress Promotes Arterial Endothelium-Oriented Differentiation of Mouse-Induced Pluripotent Stem Cells. Stem Cells International, 2019, 2019, 1-13.	2.5	10
205	Bone marrow derived endothelial progenitor cells retain their phenotype and functions after a limited number of culture passages and cryopreservation. Cytotechnology, 2019, 71, 1-14.	1.6	4
206	Effect of stress on corrosion of high-purity magnesium in vitro and in vivo. Acta Biomaterialia, 2019, 83, 477-486.	8.3	60
207	Transcatheter Selfâ€Powered Ultrasensitive Endocardial Pressure Sensor. Advanced Functional Materials, 2019, 29, 1807560.	14.9	181
208	Dynamic walking stability of elderly people with various BMIs. Gait and Posture, 2019, 68, 168-173.	1.4	12
209	The effect of pore size and porosity of Ti6Al4V scaffolds on MC3T3-E1 cells and tissue in rabbits. Science China Technological Sciences, 2019, 62, 1160-1168.	4.0	13
210	Surface modification of nanofibrous matrices via layer-by-layer functionalized silk assembly for mitigating the foreign body reaction. Biomaterials, 2018, 164, 22-37.	11.4	78
211	Crosslinking induces high mineralization of apatite minerals on collagen fibers. International Journal of Biological Macromolecules, 2018, 113, 450-457.	7.5	42
212	Effect of microporosity on scaffolds for bone tissue engineering. International Journal of Energy Production and Management, 2018, 5, 115-124.	3.7	243
213	PCSK9 regulates expression of scavenger receptors and ox-LDL uptake in macrophages. Cardiovascular Research, 2018, 114, 1145-1153.	3.8	88
214	Protective Effect of Moderate Exogenous Electric Field Stimulation on Activating Netrin-1/DCC Expression Against Mechanical Stretch-Induced Injury in Spinal Cord Neurons. Neurotoxicity Research, 2018, 34, 285-294.	2.7	7
215	Study on the formation and properties of red blood cell-like Fe <sub>3</sub> O <sub>4</sub> /TbLa <sub>3</sub> (Bim) <sub>12</sub> /PLGA composite particles. RSC Advances, 2018, 8, 12503-12516.	3.6	12
216	Influence of the quality of intraoperative fluoroscopic images on the spatial positioning accuracy of a CAOS system. International Journal of Medical Robotics and Computer Assisted Surgery, 2018, 14, e1898.	2.3	3

#	Article	IF	CITATIONS
217	Carboxylated graphene oxide promoted axonal guidance growth by activating Netrinâ€1/deleted in colorectal cancer signaling in rat primary cultured cortical neurons. Journal of Biomedical Materials Research - Part A, 2018, 106, 1500-1510.	4.0	9
218	In vitro and in vivo studies on as-extruded Mg- 5.25wt.%Zn-0.6wt.%Ca alloy as biodegradable metal. Science China Materials, 2018, 61, 619-628.	6.3	27
219	Bacteria-responsive intelligent wound dressing: Simultaneous In situ detection and inhibition of bacterial infection for accelerated wound healing. Biomaterials, 2018, 161, 11-23.	11.4	194
220	A quantitative study on magnesium alloy stent biodegradation. Journal of Biomechanics, 2018, 74, 98-105.	2.1	23
221	Potential effect of mechano growth factor E-domain peptide on axonal guidance growth in primary cultured cortical neurons of rats. Journal of Tissue Engineering and Regenerative Medicine, 2018, 12, 70-79.	2.7	8
222	Studies on Foam Decay Trend and Influence of Temperature Jump on Foam Stability in Sclerotherapy. Vascular and Endovascular Surgery, 2018, 52, 98-106.	0.7	14
223	Influence of Syringe Volume on Foam Stability in Sclerotherapy for Varicose Vein Treatment. Dermatologic Surgery, 2018, 44, 689-696.	0.8	12
224	Piezoelectric nanofibrous scaffolds as in vivo energy harvesters for modifying fibroblast alignment and proliferation in wound healing. Nano Energy, 2018, 43, 63-71.	16.0	169
225	Osteogenesis-Related Behavior of MC3T3-E1 Cells on Substrates with Tunable Stiffness. BioMed Research International, 2018, 2018, 1-10.	1.9	13
226	Patella tracking calculation from patellofemoral positions at finite angles of knee flexion. Medical Engineering and Physics, 2018, 62, 1-6.	1.7	4
227	A Novel Method to Quantify Longitudinal Orthodontic Bone Changes with In Vivo Micro-CT Data. Journal of Healthcare Engineering, 2018, 2018, 1-8.	1.9	7
228	Accuracy and reproducibility of 3D digital tooth preparations made by gypsum materials of various colors. Journal of Advanced Prosthodontics, 2018, 10, 8.	2.6	3
229	The effect of tensile and fluid shear stress on the in vitro degradation of magnesium alloy for stent applications. Bioactive Materials, 2018, 3, 448-454.	15.6	19
230	Enhancing neural differentiation of induced pluripotent stem cells by conductive graphene/silk fibroin films. Journal of Biomedical Materials Research - Part A, 2018, 106, 2973-2983.	4.0	41
231	Feasibility study on a robot-assisted procedure for tumor localization using needle-rotation force signals. Biomedical Signal Processing and Control, 2018, 46, 231-237.	5.7	0
232	A mathematical model of human heart including the effects of heart contractility varying with heart rate changes. Journal of Biomechanics, 2018, 75, 129-137.	2.1	7
233	Numerical Evaluation and Prediction of Porous Implant Design and Flow Performance. BioMed Research International, 2018, 2018, 1-13.	1.9	5
234	Fully Bioabsorbable Naturalâ€Materialsâ€Based Triboelectric Nanogenerators. Advanced Materials, 2018, 30, e1801895.	21.0	319

#	Article	IF	CITATIONS
235	Analysis of Bone Mineral Density/Content of Paratroopers and Hoopsters. Journal of Healthcare Engineering, 2018, 2018, 1-8.	1.9	2
236	Relationship between Subtalar Joint Stiffness and Relaxed Calcaneal Stance Position in Cerebral Palsy Children with Valgus Deformities. BioMed Research International, 2018, 2018, 1-10.	1.9	1
237	Static magnetic field regulates proliferation, migration, differentiation and YAP/TAZ activation of human dental pulp stem cells. Journal of Tissue Engineering and Regenerative Medicine, 2018, 12, 2029-2040.	2.7	36
238	Facile incorporation of REDV into porous silk fibroin scaffolds for enhancing vascularization of thick tissues. Materials Science and Engineering C, 2018, 93, 96-105.	7.3	17
239	Implantable Energyâ€Harvesting Devices. Advanced Materials, 2018, 30, e1801511.	21.0	214
240	Prophylactic Ankle Braces and the Kinematics and Kinetics of Half-Squat Parachute Landing. Aerospace Medicine and Human Performance, 2018, 89, 141-146.	0.4	11
241	Plantar blood flow response to accumulated pressure stimulus in diabetic people with different peak plantar pressure: a non-randomized clinical trial. Medical and Biological Engineering and Computing, 2018, 56, 1127-1134.	2.8	17
242	One-Step Preparation of Poly(Lactide-Co-Glycolide) Fiber Rods Embedding with Luminescent Materials as a Drug Delivery System via Electrospray. Nanoscience and Nanotechnology Letters, 2018, 10, 1287-1291.	0.4	9
243	Hydrolytic conversion of amorphous calcium phosphate into apatite accompanied by sustained calcium and orthophosphate ions release. Materials Science and Engineering C, 2017, 70, 1120-1124.	7.3	42
244	Improvement of hemodynamic performance using novel helical flow vena cava filter design. Scientific Reports, 2017, 7, 40724.	3.3	8
245	Preparation and characterization of electrospun graphene/silk fibroin conductive fibrous scaffolds. RSC Advances, 2017, 7, 7954-7963.	3.6	38
246	Biomechanical evaluation of the natural abutment teeth in combined tooth-implant-supported telescopic prostheses: a three-dimensional finite element analysis. Computer Methods in Biomechanics and Biomedical Engineering, 2017, 20, 967-979.	1.6	14
247	Local vibration enhanced the efficacy of passive exercise on mitigating bone loss in hindlimb unloading rats. Acta Astronautica, 2017, 137, 373-381.	3.2	16
248	Gland Instance Segmentation Using Deep Multichannel Neural Networks. IEEE Transactions on Biomedical Engineering, 2017, 64, 2901-2912.	4.2	114
249	Thermoâ€Driven Evaporation Selfâ€Assembly and Dynamic Analysis of Homocentric Carbon Nanotube Rings. Small, 2017, 13, 1603642.	10.0	11
250	Calcium concentration dependent collagen mineralization. Materials Science and Engineering C, 2017, 73, 137-143.	7.3	43
251	Shear-mediated orientational mineralization of bone apatite on collagen fibrils. Journal of Materials Chemistry B, 2017, 5, 9141-9147.	5.8	31
252	Regulating Coupling Efficiency of REDV by Controlling Silk Fibroin Structure for Vascularization. ACS Biomaterials Science and Engineering, 2017, 3, 3515-3524.	5.2	8

#	Article	IF	CITATIONS
253	Selfâ€Powered Pulse Sensor for Antidiastole of Cardiovascular Disease. Advanced Materials, 2017, 29, 1703456.	21.0	360
254	Regulation of cell arrangement using a novel composite micropattern. Journal of Biomedical Materials Research - Part A, 2017, 105, 3093-3101.	4.0	8
255	Micro-mechanical properties of different sites on woodpecker's skull. Computer Methods in Biomechanics and Biomedical Engineering, 2017, 20, 1483-1493.	1.6	6
256	The development and error analysis of a kinematic parameters based spatial positioning method for an orthopedic navigation robot system. International Journal of Medical Robotics and Computer Assisted Surgery, 2017, 13, e1782.	2.3	2
257	Biomechanical analysis of combining head-down tilt traction with vibration for different grades of degeneration of the lumbar spine. Medical Engineering and Physics, 2017, 39, 83-93.	1.7	14
258	Shear stress with appropriate time-step and amplification enhances endothelial cell retention on vascular grafts. Journal of Tissue Engineering and Regenerative Medicine, 2017, 11, 2965-2978.	2.7	13
259	Effects of different fluid shear stress patterns on the in vitro degradation of poly(lactideâ€coâ€glycolide) acid membranes. Journal of Biomedical Materials Research - Part A, 2017, 105, 23-30.	4.0	15
260	Biomechanical consideration of prosthesis selection in hybrid surgery for bi-level cervical disc degenerative diseases. European Spine Journal, 2017, 26, 1181-1190.	2.2	44
261	The Effect of Arch Height and Material Hardness of Personalized Insole on Correction and Tissues of Flatfoot. Journal of Healthcare Engineering, 2017, 2017, 1-9.	1.9	34
262	An Open-Structure Treadmill Gait Trainer: From Research to Application. Journal of Healthcare Engineering, 2017, 2017, 1-12.	1.9	1
263	User-Centric Feedback for the Development and Review of a Unique Robotic Glove Prototype to Be Used in Therapy. Journal of Healthcare Engineering, 2017, 2017, 1-8.	1.9	3
264	Biomechanical Effects of Various Bone-Implant Interfaces on the Stability of Orthodontic Miniscrews: A Finite Element Study. Journal of Healthcare Engineering, 2017, 2017, 1-10.	1.9	7
265	Parallel multiple instance learning for extremely large histopathology image analysis. BMC Bioinformatics, 2017, 18, 360.	2.6	17
266	Effect of longitudinal anatomical mismatch of stenting on the mechanical environment in human carotid artery with atherosclerotic plaques. Medical Engineering and Physics, 2017, 48, 114-119.	1.7	5
267	Calcium Hydroxide–induced Proliferation, Migration, Osteogenic Differentiation, and Mineralization via the Mitogen-activated Protein Kinase Pathway in Human Dental Pulp Stem Cells. Journal of Endodontics, 2016, 42, 1355-1361.	3.1	40
268	Hemodynamic Performance of a New Punched Stent Strut: A Numerical Study. Artificial Organs, 2016, 40, 669-677.	1.9	17
269	Electrospraying magnetic-fluorescent bifunctional Janus PLGA microspheres with dual rare earth ions fluorescent-labeling drugs. RSC Advances, 2016, 6, 99034-99043.	3.6	14
270	Enhanced osteogenic differentiation of MC3T3‣1 cells on gridâ€ŧopographic surface and evidence for involvement of YAP mediator. Journal of Biomedical Materials Research - Part A, 2016, 104, 1143-1152.	4.0	31

#	Article	IF	CITATIONS
271	Current investigations into magnetic nanoparticles for biomedical applications. Journal of Biomedical Materials Research - Part A, 2016, 104, 1285-1296.	4.0	248
272	The effect of fluid shear stress on the <i>in vitro</i> degradation of poly(lactideâ€ <i>co</i> â€glycolide) acid membranes. Journal of Biomedical Materials Research - Part A, 2016, 104, 2315-2324.	4.0	24
273	Cross-Talk Between PCSK9 and Damaged mtDNA in Vascular Smooth Muscle Cells: Role in Apoptosis. Antioxidants and Redox Signaling, 2016, 25, 997-1008.	5.4	63
274	Apparent- and Tissue-Level Yield Behaviors of L4 Vertebral Trabecular Bone and Their Associations with Microarchitectures. Annals of Biomedical Engineering, 2016, 44, 1204-1223.	2.5	16
275	Hydroxyapatite-containing silk fibroin nanofibrous scaffolds for tissue-engineered periosteum. RSC Advances, 2016, 6, 19463-19474.	3.6	18
276	The effects of fluid shear stress on proliferation and osteogenesis of human periodontal ligament cells. Journal of Biomechanics, 2016, 49, 572-579.	2.1	26
277	The effects of tensile stress on degradation of biodegradable PLGA membranes: A quantitative study. Polymer Degradation and Stability, 2016, 124, 95-100.	5.8	46
278	Silk scaffolds for musculoskeletal tissue engineering. Experimental Biology and Medicine, 2016, 241, 238-245.	2.4	48
279	Shear-mediated crystallization from amorphous calcium phosphate to bone apatite. Journal of the Mechanical Behavior of Biomedical Materials, 2016, 54, 131-140.	3.1	35
280	Simulated bone remodeling around tilted dental implants in the anterior maxilla. Biomechanics and Modeling in Mechanobiology, 2016, 15, 701-712.	2.8	19
281	Three-dimensional quantification of orthodontic root resorption with time-lapsed imaging of micro-computed tomography in a rodent model. Journal of X-Ray Science and Technology, 2015, 23, 617-626.	1.0	8
282	Comparison of Postural Responses to Galvanic Vestibular Stimulation between Pilots and the General Populace. BioMed Research International, 2015, 2015, 1-6.	1.9	19
283	Hemodynamic Shear Stress <i>via</i> ROS Modulates PCSK9 Expression in Human Vascular Endothelial and Smooth Muscle Cells and Along the Mouse Aorta. Antioxidants and Redox Signaling, 2015, 22, 760-771.	5.4	160
284	Biomechanical behavior of valgus foot in children with cerebral palsy: A comparative study. Journal of Biomechanics, 2015, 48, 3170-3177.	2.1	9
285	Does Location of Rotation Center in Artificial Disc Affect Cervical Biomechanics?. Spine, 2015, 40, E469-E475.	2.0	54
286	Effect of nanoâ€hydroxyapatiteâ€coated magnetic nanoparticles on axonal guidance growth of rat dorsal root ganglion neurons. Journal of Biomedical Materials Research - Part A, 2015, 103, 3066-3071.	4.0	16
287	Delivery of demineralized bone matrix powder using a salt-leached silk fibroin carrier for bone regeneration. Journal of Materials Chemistry B, 2015, 3, 3177-3188.	5.8	25
288	Biomechanical effects of corticotomy approaches on dentoalveolar structures during canine retraction: A 3-dimensional finite element analysis. American Journal of Orthodontics and Dentofacial Orthopedics, 2015, 148, 457-465.	1.7	30

#	Article	IF	CITATIONS
289	Physiological Significance of Helical Flow in the Arterial System and its Potential Clinical Applications. Annals of Biomedical Engineering, 2015, 43, 3-15.	2.5	118
290	Greater scaffold permeability promotes growth of osteoblastic cells in a perfused bioreactor. Journal of Tissue Engineering and Regenerative Medicine, 2015, 9, E210-E218.	2.7	24
291	Influence of Mechanical Fixation on Angiogenesis during Bone Healing Process. IFMBE Proceedings, 2015, , 111-113.	0.3	1
292	Simulation of Contrast Agent Transport in Arteries with Multilayer Arterial Wall: Impact of Arterial Transmural Transport on the Bolus Delay and Dispersion. Scientific World Journal, The, 2014, 2014, 1-13.	2.1	1
293	3D-Printed Biopolymers for Tissue Engineering Application. International Journal of Polymer Science, 2014, 2014, 1-13.	2.7	103
294	In vivo measurements of patellar tracking and finite helical axis using a static magnetic resonance based methodology. Medical Engineering and Physics, 2014, 36, 1611-1617.	1.7	10
295	Effects of hydroxyapatite/collagen composite on osteogenic differentiation of rat bone marrow derived mesenchymal stem cells. Journal of Composite Materials, 2014, 48, 1971-1980.	2.4	16
296	Physiological pulsatile flow culture conditions to generate functional endothelium on a sulfated silk fibroin nanofibrous scaffold. Biomaterials, 2014, 35, 4782-4791.	11.4	52
297	Effect of fixation on neovascularization during bone healing. Medical Engineering and Physics, 2014, 36, 1436-1442.	1.7	14
298	Biomechanical investigation of thoracolumbar spine in different postures during ejection using a combined finite element and multiâ€body approach. International Journal for Numerical Methods in Biomedical Engineering, 2014, 30, 1121-1131.	2.1	49
299	A Mechanical Model of the Cornea Considering the Crimping Morphology of Collagen Fibrils. , 2014, 55, 2739.		63
300	Reliability and Validity of Kinect RGB-D Sensor for Assessing Standing Balance. IEEE Sensors Journal, 2014, 14, 1633-1638.	4.7	79
301	A histological and biomechanical study of bone stress and bone remodeling around immediately loaded implants. Science China Life Sciences, 2014, 57, 618-626.	4.9	13
302	Numerical simulation of the remodelling process of trabecular architecture around dental implants. Computer Methods in Biomechanics and Biomedical Engineering, 2014, 17, 286-295.	1.6	10
303	Biocomposites reinforced by fibers or tubes as scaffolds for tissue engineering or regenerative medicine. Journal of Biomedical Materials Research - Part A, 2014, 102, 1580-1594.	4.0	103
304	Effect of substrate stiffness on the functions of rat bone marrow and adipose tissue derived mesenchymal stem cells <i>in vitro</i> . Journal of Biomedical Materials Research - Part A, 2014, 102, 1092-1101.	4.0	91
305	Nitric Oxide Transport in Normal Human Thoracic Aorta: Effects of Hemodynamics and Nitric Oxide Scavengers. PLoS ONE, 2014, 9, e112395.	2.5	16
306	Geometric classification of the carotid siphon: association between geometry and stenoses. Surgical and Radiologic Anatomy, 2013, 35, 385-394.	1.2	23

#	Article	IF	CITATIONS
307	Involvement of large conductance Ca2+-activated K+ channel in laminar shear stress-induced inhibition of vascular smooth muscle cell proliferation. Pflugers Archiv European Journal of Physiology, 2013, 465, 221-232.	2.8	25
308	Biomechanism of impact resistance in the woodpecker's head and its application. Science China Life Sciences, 2013, 56, 715-719.	4.9	31
309	Potential protective effect of biphasic electrical stimulation against growth factor-deprived apoptosis on olfactory bulb neural progenitor cells through the brain-derived neurotrophic factor–phosphatidylinositol 3′-kinase/Akt pathway. Experimental Biology and Medicine, 2013, 238, 951-959.	2.4	23
310	Numerical simulation of nucleotide transport in the human thoracic aorta. Journal of Biomechanics, 2013, 46, 819-827.	2.1	8
311	Increased Proliferation and Differentiation of Pre-Osteoblasts MC3T3-E1 Cells on Nanostructured Polypyrrole Membrane Under Combined Electrical and Mechanical Stimulation. Journal of Biomedical Nanotechnology, 2013, 9, 1532-1539.	1.1	25
312	Multi-label classification for colon cancer using histopathological images. Microscopy Research and Technique, 2013, 76, 1266-1277.	2.2	28
313	Relationship between Microstructure, Material Distribution, and Mechanical Properties of Sheep Tibia during Fracture Healing Process. International Journal of Medical Sciences, 2013, 10, 1560-1569.	2.5	14
314	Nitric oxide transport in an axisymmetric stenosis. Journal of the Royal Society Interface, 2012, 9, 2468-2478.	3.4	23
315	Galvanic Vestibular Stimulation and the Ability to Maintain Arm-Hand Posture. Aviation, Space, and Environmental Medicine, 2012, 83, 654-659.	0.5	4
316	Effect of nano-hydroxyapatite on the axonal guidance growth of rat cortical neurons. Nanoscale, 2012, 4, 3201.	5.6	29
317	Micro-/Nano- sized hydroxyapatite directs differentiation of rat bone marrow derived mesenchymal stem cells towards an osteoblast lineage. Nanoscale, 2012, 4, 2484.	5.6	88
318	Nano-hydroxyapatite particles induce apoptosis on MC3T3-E1 cells and tissue cells in SD rats. Nanoscale, 2012, 4, 2894.	5.6	50
319	Flow patterns and wall shear stress distribution in human internal carotid arteries: The geometric effect on the risk for stenoses. Journal of Biomechanics, 2012, 45, 83-89.	2.1	65
320	Fluid shear stress regulates metalloproteinase-1 and 2 in human periodontal ligament cells: Involvement of extracellular signal-regulated kinase (ERK) and P38 signaling pathways. Journal of Biomechanics, 2012, 45, 2368-2375.	2.1	37
321	Effect of Cyclic Strain on Cardiomyogenic Differentiation of Rat Bone Marrow Derived Mesenchymal Stem Cells. PLoS ONE, 2012, 7, e34960.	2.5	72
322	Comparative study of Newtonian and non-Newtonian simulations of drug transport in a model drug-eluting stent. Biorheology, 2012, 49, 249-259.	0.4	13
323	Relationships Between Femoral Strength Evaluated by Nonlinear Finite Element Analysis and BMD, Material Distribution and Geometric Morphology. Annals of Biomedical Engineering, 2012, 40, 1575-1585.	2.5	38
324	The use of carbon nanotubes to induce osteogenic differentiation of human adipose-derived MSCs inÂvitro and ectopic bone formation inÂvivo. Biomaterials, 2012, 33, 4818-4827.	11.4	250

#	Article	IF	CITATIONS
325	Improved Hemocompatibility and Endothelialization of Vascular Grafts by Covalent Immobilization of Sulfated Silk Fibroin on Poly(lactic-co-glycolic acid) Scaffolds. Biomacromolecules, 2011, 12, 2914-2924.	5.4	83
326	A novel deployment design of vena cava filters might be the solution to their blockage problem. Medical Hypotheses, 2011, 77, 990-992.	1.5	1
327	Repair of Bone Defect in Femoral Condyle Using Microencapsulated Chitosan, Nanohydroxyapatite/Collagen and Poly(L‣actide)â€Based Microsphereâ€Scaffold Delivery System. Artificial Organs, 2011, 35, E119-28.	1.9	48
328	Effect of the endothelial glycocalyx layer on arterial LDL transport under normal and high pressure. Journal of Theoretical Biology, 2011, 283, 71-81.	1.7	41
329	Electrospun sulfated silk fibroin nanofibrous scaffolds for vascular tissue engineering. Biomaterials, 2011, 32, 3784-3793.	11.4	192
330	Effect of non-Newtonian and pulsatile blood flow on mass transport in the human aorta. Journal of Biomechanics, 2011, 44, 1123-1131.	2.1	155
331	MICRO-FINITE ELEMENT ANALYSIS OF TRABECULAR BONE YIELD BEHAVIOR — EFFECTS OF TISSUE NONLINEAR MATERIAL PROPERTIES. Journal of Mechanics in Medicine and Biology, 2011, 11, 563-580.	0.7	17
332	Why Do Woodpeckers Resist Head Impact Injury: A Biomechanical Investigation. PLoS ONE, 2011, 6, e26490.	2.5	120
333	Biomechanical Gender Differences of the Ankle Joint During Simulated Half-Squat Parachute Landing. Aviation, Space, and Environmental Medicine, 2010, 81, 761-767.	0.5	25
334	Effect of Fluid Shear Stress on Cardiomyogenic Differentiation of Rat Bone Marrow Mesenchymal Stem Cells. Archives of Medical Research, 2010, 41, 497-505.	3.3	109
335	Endothelium oriented differentiation of bone marrow mesenchymal stem cells under chemical and mechanical stimulations. Journal of Biomechanics, 2010, 43, 1176-1181.	2.1	98
336	Influences of tensile load on in vitro degradation of an electrospun poly(l-lactide-co-glycolide) scaffold. Acta Biomaterialia, 2010, 6, 2991-2996.	8.3	59
337	Current investigations into carbon nanotubes for biomedical application. Biomedical Materials (Bristol), 2010, 5, 022001.	3.3	108
338	A Dual-Frequency Loading Device for Tissue Engineering Cartilage. International Conference on Bioinformatics and Biomedical Engineering: [proceedings] International Conference on Bioinformatics and Biomedical Engineering, 2010, , .	0.0	0
339	A numerical study on the flow of blood and the transport of LDL in the human aorta: the physiological significance of the helical flow in the aortic arch. American Journal of Physiology - Heart and Circulatory Physiology, 2009, 297, H163-H170.	3.2	159
340	The influence of mechanical loading on osseointegration: an animal study. Science in China Series C: Life Sciences, 2009, 52, 579-586.	1.3	5
341	Formation of porous PLGA scaffolds by a combining method of thermally induced phase separation and porogen leaching. Journal of Applied Polymer Science, 2008, 109, 1232-1241.	2.6	69
342	An S-type bypass can improve the hemodynamics in the bypassed arteries and suppress intimal hyperplasia along the host artery floor. Journal of Biomechanics, 2008, 41, 2498-2505.	2.1	47

#	Article	IF	CITATIONS
343	In vitro degradation of porous poly(l-lactide-co-glycolide)/l²-tricalcium phosphate (PLGA/l²-TCP) scaffolds under dynamic and static conditions. Polymer Degradation and Stability, 2008, 93, 1838-1845.	5.8	91
344	Numerical simulation of tooth movement in a therapy period. Clinical Biomechanics, 2008, 23, S48-S52.	1.2	40
345	Development of a finite element model of female foot for high-heeled shoe design. Clinical Biomechanics, 2008, 23, S31-S38.	1.2	115
346	Biomechanical and histological evaluation of the application of biodegradable poly-l-lactic cushion to the plate internal fixation for bone fracture healing. Clinical Biomechanics, 2008, 23, S7-S16.	1.2	49
347	Fitting Curve Passing through Designated Point to Data for Promoting the Reproducibility of Peripheral Quantitative Computed Tomography (pQCT). , 2008, , .		0
348	The Proliferation and Gene Expression in MC3T3-E1 under Simulated Microgravity. , 2007, , .		1
349	Intelligibility of Mandarin Speech Produced Using Different Vocal Rehabilitation Technique in Quiet and in Noise. , 2007, , .		0
350	Reconstruction of Three-dimensional Model of Normal Female Pelvic Cavity Based on Magnetic Resonance Imaging. , 2007, , .		2
351	Comparative Study on Biological Effects of Two-Dimensional and Three-Dimensional Simulated Microgravity. , 2007, , .		0
352	The potential of Triptolide as effective topical anti-inflammatory agent. , 2007, , .		0
353	Clinical Efficacy of Traditional Chinese Medicine for COVID-19: A Systematic Review and Meta-Analysis. SSRN Electronic Journal, 0, , .	0.4	0
354	Biomechanical effect of posterior ligament repair in lamina repair surgery. Computer Methods in Biomechanics and Biomedical Engineering, 0, , 1-8.	1.6	0